HYDROGEN, FUEL CELL & ENERGY STORAGE

Thermoexergetic analysis of common rail direct injection diesel engine on optimized multiple injection strategy of performance and emission using congress grass tamarind shell co-pyrolysis oil blend and diesel

T. Sreenivasa Murthy[a,*] | **B. Jayachandraiah**[b] | **B. Durga Prasad**[a]

[a] Department of Mechanical Engineering, Jawaharlal Nehru Technological university, Anantapur-515002, Andhra Pradesh, India
[b] Department of Mechanical Engineering, Sri kalahasteeswara Institute of Technology, Srikalahasti-517640, Andhra Pradesh, India
[*] Corresponding author, Email: tsreem@gmail.com

Article Information

Article Type
Research Article

Article History
Received: *30 Feb 2024*
Revised: *15 May 2024*
Accepted: *02 Jun 2024*
Published Online: *05 Jun 2024*

Keywords
Energy
Exergy
Injection timing
Emissions
Injection duration
Optimization

Abstract

Internal combustion engine energy and exergy analysis is essential when choosing a biofuel that can be used as an alternative to conventional diesel, as these analyses provide concerns about the quantity and quality of available energy. In this study, the multiple injection strategies (MIS) in an improved common rail direct injection (CRDI) diesel engine running on 20% blend of Congress grass Tamarind shell co-pyrolysis oil (CGTSCPO20) and diesel is optimized and energy and exergy analysis has been made at optimized condition. The optimal result reveals that there was a slight improvement in brake thermal efficiency (BTE) and reduction in emissions. By increasing the IOP from 600 bar to 1100 bar with the same fuel IT of 10° bTDC, the performance is enhanced. Studies reveal that, apart from nitrogen oxides (NO_x), emissions decrease under ideal circumstances of 80% load and 1000 bar pressure when brake thermal efficiency (BTE) increases. From the experimental results, it was observed that destruction of exergy for CGTSCPO20 and diesel were 59.24% and 50.17%, respectively.

Cite this article: Murthy, T. S., Jayachandraiah, B., Prasad, B. D. (2024). Thermoexergetic analysis of common rail direct injection diesel engine on optimized multiple injection strategy of performance and emission using congress grass tamarind shell co-pyrolysis oil blend and diesel. DOI: 10.22104/HFE.2024.6643.1281

 Publisher: Iranian Research Organization for Science and Technology (IROST)
DOI: 10.22104/HFE.2024.6643.1281

1 Introduction

In the present situation with huge demand of fossil fuel results in increasing cost of fossil fuels, their rapid depletion and contribution to environmental pollution focuses on search of alternative fuels. Biomass energy is emerging as a desirable and sustainable substitute fuel option for diesel engines, among the various alternative fuels that are now accessible [1]. Several processes, such as pyrolysis, anaerobic digestion, transesterification, and liquefaction, can be used to convert biomass into energy in the form of liquid fuels [2–4]. It was discovered that pyrolysis was a very practical and alluring process for extracting oil from any type of biomass that was accessible. Many researchers have been interested in the pyrolysis of a wide range of biomasses [5].

Pyrolysis can be defined as the thermal degradation of biomass that takes place in the absence of air/oxygen; the process results in the production of three distinct types of products, including volatile gases, solids (bio-char) and liquids (bio-oil). Pyrolysis oil, often known as bio-oil, is the name given to the liquid product of the pyrolysis process. This substance is an organic liquid that is a dark brown colour, and it can be used as fuel in many different applications. Additionally, it can be used as a raw material in the production of hydrocarbons and it can easily be connected to oil refineries that already exist in operation or to bio refineries that will be built in the future [6].

The only distinction between co-pyrolysis and pyrolysis is that co-pyrolysis uses two or more different chemicals. By using co-pyrolysis, one can improve the production of bio-oil, lower its water content, increase its calorific value, and modify the chemical structure and physical characteristics of the pyrolysis products. Many researchers have worked on co-pyrolysis to improve the quality and quantity of bio-oil produced during pyrolysis. Co-pyrolysis requires a thorough understanding of the synergistic effects of basic components. There are numerous reports that biomass pyrolysis produces bio-oil with higher yield and requires quality than pyrolysis [7–9]. There is a lot of information in the literature about various pyrolysis methods for biomass sources like agricultural waste materials, wood, wood waste, wheat straw, rice straw, EFB, seeds of biomass, and manures.

The current research on the generation of energy aims to develop the methods of energy production that are not only inexpensive but also environmentally friendly and sustainable. Alternatives to crude oil that are made from biomass like wood [10, 11] and agricultural products [12–15] have shown a lot of promise. The fact that the production of high-value crops and biomass are in direct conflict with one another is one of the most significant drawbacks of using huge amounts of biomass for energy [16].

Energy and exergy analysis may be used to understand the engine performance in terms of energy output. Because the constraints of the second law of thermodynamics are not taken into account, analysis based on the first law of thermodynamics is inadequate to explain fuel sustainability. Renewability and sustainability are strongly connected to another variable, exergy, which is computed using both the first and second laws of thermodynamics. An effective way to understand the instability of a thermodynamic system for converting energy is via exergy analysis. As a way to deal with the issues raised by the widespread use of different energy sources and the resulting environmental issues, it has become more and more popular lately [17–21]. As recently reported and discussed below, researchers have also utilized exergy analysis to assess and optimize the performance of internal combustion engines (IC) operating on non-renewable and renewable fuels and mixes thereof.

For a diesel engine running on diesel, methyl soybean oil, and high oleic soybean oil, Caliskan et al. performed energy and exergy evaluations [22]. Canakci and Hosoz [23] employed exergy analysis to evaluate the efficiency of a four-cylinder turbodiesel engine that was operated on various fuels, including gasoline and biodiesel. Using energy and exergy analysis, Da Costa et al. investigated the efficiency of a dual-fuel diesel engine that works on both natural gas and diesel [24]. Lopez et al. reported on their exergy performance analysis of diesel engines utilizing diesel fuel, biodiesel made from olive pomace oil, and their blends [25]. Sekmen and Yilbasi examined the energy and exergy properties of diesel and soybean biodiesel in a four-cylinder direct injection diesel engine [26].

The study conducted by Biplab et al. investigated the effects of injection duration and compression ratio on energy and exergy potential in a diesel engine that was powered by palm oil methyl ester [27]. Panigrahi et al. reported on the energy and exergy research of a diesel engine using Mahua biodiesel in addition to diesel [28].

Panigrahi et al. conducted an energy and exergy analysis on diesel mixed fuel for diesel engines with 20% neem oil methyl ester. They discovered that the blended fuel had reduced exhaust energy loss and greater heat transfer rate, so it was shown to be equivalence to diesel fuel. Energy and performance trends for different fuels are comparable [29]. In Karagoz et al.'s study, the blends made of diesel and tire-pyrolysis oil were used to study the energy, efficiency, and economy of diesel engines. The maximum energy and exergy

efficiency was shown to be attained at 10% pyrolysis oil [30].

The impact of nanoparticle concentration on the energy and exergy efficiency of diesel engines was investigated by Karami and Gharehghan. B0W5N60, which contains 60 ppm of nano particles and 5% water, was shown to have better thermal efficiency than pure diesel [31]. When employing diesel-biodiesel blends including various metal oxide nanoparticles, Kargoz et al. conducted exergy and exergy economics analyses of diesel engines, demonstrating that nano fuel performs better than both regular diesel fuel and diesel-biodiesel blends [30]. From their research on energy and exergy of non-edible biodiesel blends in direct injection diesel engines, Nabia and Rasul found that the exergy parameters of biodiesel blends were only marginally different from those of reference diesel [32].

The B20 blend has the greatest exergy efficiency, according to Nemati et al.'s analysis of the exergy efficiency of diesel engines using biodiesel and its blends [33]. Sarikoc et al. studied the energy and exergy of diesel engines using different mixtures of diesel, biodiesel and butanol fuels. They found that the butanol combination had greater energy and energy efficiency than diesel [34]. With diesel and biodiesel fuels, Sanli and Uludamar investigated the energy output and efficiency of diesel engines operating at various speeds. They discovered that the usage of biodiesel lowers fuel exergy and energy efficiencies [35]. Yesilyurt and Arslan investigated how various injector pressures affected the power and energy effectiveness of diesel engines operating at a constant speed. Yesilyurt and Arslan's findings revealed that the maximum energy efficiency is 24.51% and the highest exergy efficiency is 21.27% at a pressure of 190 bar [36]. Particularly when utilising diesel and biodiesel mixtures, injection time and pressure are important factors impacting the performance of diesel engines [37–41].

Common Rail Direct Injection (CRDI) system employs high-pressure common rail fuel injection and electronic control unit (ECU), which has the ability to accomplish effective air-fuel mixing, regulated ignition, and combustion, consequently decreasing emissions from diesel engines. It permits adjustable control of injector pressure, amount of fuel injected, and injection time [42]. Common Rail Direct Injection (CRDI) systems may raise injection pressures up to 1900 bar, making diesel engines cleaner, quieter, and more environmental friendly [43].

Indrareddy et al. [44] described a CRDI system for diesel engines in which the utilisation of diesel and biodiesel mixes with alumina nanoparticles dramatically decreased specific fuel consumption as well as HC and smog emissions. According to Syed and Servanan, CRDI systems are anticipated to greatly decrease specific fuel consumption and soot emissions compared to traditional diesel engines; however, NO_x emissions are on the rise. They found that combining algal biodiesel with diesel decreased HC emissions and smoke opacity while increasing NO_x emissions in a CRDI engine fuelled by algae biodiesel [45]. Khandal et al. demonstrated that the thermal efficiency of the brakes increased when the CRDI engine was run at 900 bar internal air pressure and 10 degrees bTDC fuel injection timing [46].

Based on prior research, it can be stated that energy and exergy analysis helps determine ideal operating conditions, such as engine parameters and fuel blends, and helps comprehend how alternative fuels perform in order to design more economical and environmentally friendly operations. Research on the interaction between CRDI engine performance and other tuning parameters, such as fuel, showed that these parameters enhanced engine performance and reduced emissions [47–49].

1.1 The objective of the current study

From extensive literature review, it has been observed that there are no studies on energy and exergy of CRDI engine configurations utilising bio-oil made from congress grass (CG) and tamarind shell (TS) co-pyrolysis oil as fuel. The unique aspect of this research is how the second law of thermodynamics is used to examine the usage of congress grass and tamarind shell co-pyrolysis oil as alternative fuels for CRDI engines under ideal operating conditions.

The purpose of the current study is to use energy and exergy as most effective tool to evaluate the performance of CRDI engine under optimised load, ignition timing and ignition pressure conditions, as well as to optimize timing of injection and injector pressure to enhance the overall efficiency by utilising TRCC combustion chamber with 7-hole injectors by comparing energy, exergy, performance and emissions characteristics, using co-pyrolysis oil blend (CGTSCPO20) as biofuel and diesel.

1.2 Novelty of present research

- New co-pyrolysis oil from bio product has been prepared and tested in CRDI engine.
- Energy availability and optimal conversion into useful work has been analysed.
- Impact of injection timing and injector opening pressure on performance and emission has been studied and compared to optimize the overall efficiency of the engine.

2 Experimental

2.1 Preparation of test fuel

The collected tamarind shell is dried in sunlight for a few days and the Congress grass (Parthenium hysterophorus) is collected, cut into 8-10 mm pieces, and dried in the sun for a few days. Figures 1 and 2 show congress grass and tamarind shell. The collected dried raw material was fed in a 1 : 1 ratio to a fixed bed reactor shown in Figure 3 and pyrolysis was performed up to an operating temperature of 500 °C.

The reaction was allowed to proceed for nearly 4 hours at atmospheric pressure, after which the pyrolysis products were condensed and the pyrolysis oil was collected and refined liquid-liquid with hexane. Refined pyrolysis oil is mixed with diesel in a mass ratio of 20%. After 2 hours, the emulsion was found to be stable without phase separation. The physicochemical properties of pure diesel oil, pure co-pyrolysis oil and mixed test samples were determined by standard ASTM methods and are shown in Table 1, the table shows that all the quiescent physicochemical properties are within ASTM standards.

Table 1 summarizes the characteristics of pure CGTSCPO and its 20% blend with diesel (CGTSCPO20). It is noticeable that 20% blend bio-oil has a lower viscosity and a higher calorific value. This suggests that this bio-oil can be used effectively as fuel in CI engines. However, the higher amount of water and lower pH value suggests that the raw CGTSCPO needs to be improved before it can be used as an alternative to fossil fuels.

2.2 Methodology of experimentation

Initially on a CRDI engine fuelled with CGTSCPO20 and diesel, experimental tests were conducted to study the performance and emissions at 80% and 100% load, the IT was changed from 25° bTDC to 5° aTDC with a step of 5°, while the IOP remained constant at 600 bar. A Delta 1600S exhaust gas analyser was used to check HC, CO and NO_x levels.

The amount of smoke that was released was determined with the help of a Hartridge smoke meter. In the second part, experiments were conducted using the same equipment and blends in order to optimise the IOP, which ultimately results in improved performance. In order to optimize the pressure variation, tests were performed at 600, 700, 900, 1000, and 1100 bar, while an optimal IT of 10° bTDC was maintained throughout. The investigation was extended further to analyze the energy and exergy at optimized conditions for IOP and IT with the same device and fuels.

Fig. 1. Congress grass

Fig. 2. Tamarind shell

Table 1. Physiochemical properties of raw CGTSCPO bio-oil and B20 blend.

Property	Pure CGTSCPO	Blended CGTSCPO20
Kinematic viscosity (Cst) at 40 °C	10.7	4.2
Calorific value (MJ/kg)	38.1	43.1
Cetane number	41	47
Density at 30 °C (g/cc)	1.08	0.89
Flash point (°C)	85	73
Fire point (°C)	103	85
pH	3.9	5.3
Pour point (°C)	9.1	−4.9
Moisture content (weight%)	19.6	4.1

2.3 Engine setup

Figure 3 represents the engine setup with all equipment. Suitable modifications have been made in test engine with power output of 5.2 kW for successful running on common rail direct injection principle more injector pressure. Figure 4 represents the electronic control unit which controls the common rail direct injection system. The ECU system simplifies the operation of CRDI engine biodiesel injection under various IT and IOP. Engine details are given in Table 2. Figures 5 and 6 shows a Hatridge smoke meter used to determine smoke and a five-gas analyzer (DELTA 1600 S-NDIR Analyzers). Tables 3 and 4 below list the most important specifications for smoke meters and exhaust gas analyzers.

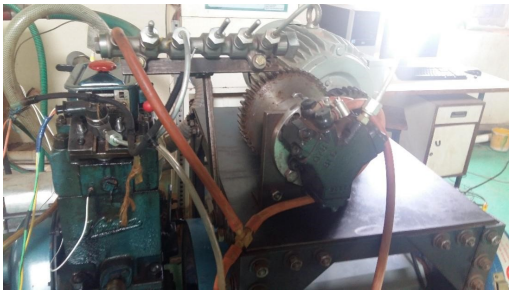

Fig. 3. Experimental setup

Fig. 4. Electronic control unit.

Table 2. Engine specification.

Parameter	Specification
Engine type	Kirloskar make, single cylinder 4 stroke, Direct injection diesel engines
Nozzle opening pressure	205 bar
Power	5.2kW@1500rpm
Bore	87.5
Stroke	110
Compression ratio	17.5:1
Injection timing	23° TDC
Type of cooling	Water

Fig. 5. Five gas analyser.

Fig. 6. Hartridge smoke meter.

Table 3. Smoke meter specification.

Type	Hartridge Smokemeter - 4
Measuring range	0 - 100 %
Resolution	0.10%
Accuracy	±2% relative
Smoke length	0.43 m
Ambient temperature range	−5 °C - +45 °C
Warm up duration	10 min at 20 °C
Power supply	100 to 240 V AC/50 Hz 10-16 V DC @15 amps
Size	100 mm × 210 mm × 50 mm.

Table 4. Specifications of the five-gas analyser.

	HC	CO	CO_2	O_2	NO_x
Measuring range	0 to 20000 ppm as C_3H_8 (propane)	0 to 10%	0 to 16%	0 to 21%	0 to 5000 ppm (as nitric oxide)
Accuracy	±30 ppm HC	±0.2%	±1%	±0.2%	±10 ppm NO_x
Resolution	1ppm	0.01% volume	0.1% volume	0.01% volume	1 ppm

2.4 Theoretical basis for the analysis of the 1st and 2nd law of thermodynamics

Not all of the engine's heat energy is turned into braking power. Friction, radiation, mixing losses, fluid flow losses, combustion losses, throttling losses in intake and exhaust, and other factors are taken into consideration when calculating the input energy. It would undoubtedly be wise to investigate the many mechanisms via which the engine's heat energy is converted into useful work or lost. By using the first law of thermodynamics, this is made possible. Engine performance could be enhanced by analysing the energy equal to braking power, heat removed by cooling water, heat removed by exhaust gases, and unaccounted heat losses at different engine loads.

The mathematical equations (1)-(5) usually used to estimate these quantities are presented below [50, 51].

$$Q_i = m_f \times \mathrm{LCV}\,, \tag{1}$$

$$Q_{bp} = \frac{2\pi NT}{60000}\,, \tag{2}$$

$$Q_w = m_w C_w \left(T_{co} - T_{ci}\right), \tag{3}$$

$$Q_e = m_e\, C_e \left(T_e - T_a\right), \tag{4}$$

$$Q_L = Q_i - \left(Q_{bp} + Q_w + Q_e\right), \tag{5}$$

where Q_i is input heat energy in kJ, m_f is mass of fuel in kg, LCV is lower calorific value of fuel in kJ/kg, Q_{bp} is heat equivalent to brake power in kJ, N is speed in RPM, T is torque in N · m, Q_w is heat carried away by cooling water in kJ, m_w is mass of water (kg), C_w is specific heat of cooling water in kJ/kg · K, C_e is specific heat of exhaust gas in kJ/kg · K, T_{ci} is temperature of cooling water at inlet in K, T_{co} is temperature of cooling water at outlet in K, Q_e is heat carried away by exhaust gases in kJ, Q_L unaccounted losses, m_e is mass of exhaust gas (kg).

The transfer of brake power availability, cooling water availability, and exhaust gas availability results from the fuel input's available energy (exergy). The unaccounted losses account for most of the availability is lost. It is possible to compute this availability of (exergy) transfer by applying the second law of thermodynamics. The chemical availability of fuel (A_i) was calculated using equation (6). The quantity of heat equal to the brake power (A_{bp}) and the availability corresponding to it are identical by nature. Equations (8)-(10) were used to determine additional values, such as availability in cooling water (A_w), exhaust gases (A_e), and availability lost owing to unaccounted losses (A_L).

$$A_i = 1.0338\, Q_i\,, \tag{6}$$

$$A_{bp} = Q_{bp}\,, \tag{7}$$

$$A_w = Q_w - T_a \left[m_w C_w \ln\left(\frac{T_{co}}{T_{ci}}\right)\right], \tag{8}$$

$$A_e = Q_e - mT_a \left[C_e \ln\left(\frac{T_a}{T_e}\right) - R_e \ln\left(\frac{P_a}{P_e}\right)\right], \tag{9}$$

$$A_L = A_i - \left(A_{bp} + A_w + A_e\right), \tag{10}$$

where, A_i is fuel availability in kW, A_{bp} is shaft availability in kW, A_w is cooling water availability in kW, A_e is exhaust availability in kW, A_L is destruction in kW, T_{co} is cooling water temperature K, m_w is mass of cooling water circulating through the cooling jacket in kg, C_w is specific heat of water in kJ/kg · K, T_{ci} is inlet water temperature through the cooling jacket in K, T_{co} is outlet water temperature of the cooling jacket in K, T_a is ambient temperature in K, R_e is specific gas constant of exhaust gas, unit is kJ/kg K, P_a is ambient pressure in N/m^2, P_e is final pressure in N/m^2, m_g is mass of exhaust gas in kg, T_e is exhaust gas temperature in K. The exhaust gas molecular weight was assumed to be 28.75 g/mol. In the above-mentioned molecular weight, the characteristic gas constant (R_e) would be 0.287 kg/K.

3 Results and discussion

3.1 IT Optimization in the CRDI engine for the diesel and CGTSCPO20 fuels

For fuel IT optimization of CRDI diesel engines, extensive tests were conducted on engine setup using tested fuels. Toroidal re-entrant combustion chamber was selected for the experiment, and the engine runs at fixed speed of 1500 RPM. Optimized injection time of fuel was set in 5° CA steps, within range of 25° crank

angle before top dead centre to 5° crank angle after top dead centre at 80% and full load conditions. The 600 bar injector opening pressure in CRDI engine was kept constant by using CRDI fuel injectors with 7 holes of 0.2 mm diameter. For the investigation, engine loads of 80% and full load were selected and performance and emission parameters were evaluated and compared.

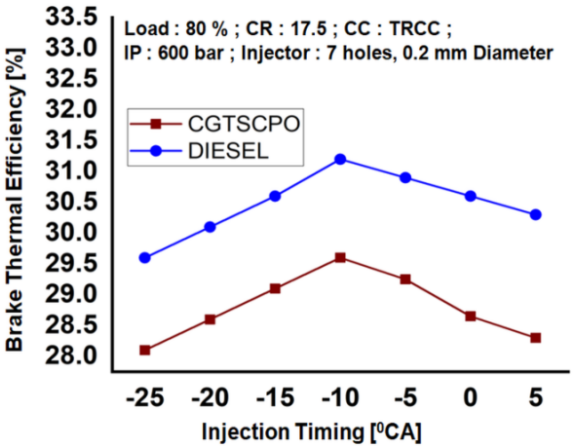

(a)

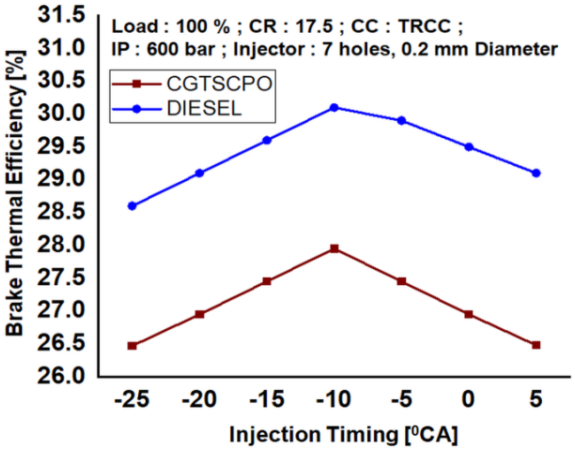

(b)

Fig. 7. Variation in the BTE for 80% and full load conditions at different ITs for diesel and CGTSCPO20.

3.1.1 Impact of injection time on BTE

Figure 7 depict the impact of injection timing in a CRDI engine using diesel fuel and CGTSCPO20 at 80% and full load. According to the findings, the pyrolysis oil's maximum BTE was revealed at 10° bTDC. This is because of better atomization at 600 bar pressure. Improved mixing of fuel is another factor contributing to higher BTE. The decrease in time of walls wetting increases fuel burning rate and rises BTE of the engine running with CGTSCPO20 oil. The CRDI engine can modify the brake thermal efficiency by either retarding or advancing injection timing. As the IT is retarded, the BTE is decreased. This is due to the increased amount of fuel being delivered into the crevice, reducing the time available for air fuel mixing. This leads to a lower overall BTE. When engine was loaded to 80% capacity, the BTE for CGTSCPO20 and diesel, respectively, came in at 28 and 30.65% at 10° bTDC IT. Similarly, at full load, CGTSCPO20 and diesel generated respective efficiencies of 27.5% and 30% at 10° bTDC IT. The results showed that at 80% load and 10° bTDC IT in a CRDI engine with a 7-hole CRDI injector and a combustion chamber in the shape of a TRCC with a 600 bar IOP, diesel had a greater BTE than CGTSCPO20 oil for its low viscosity and higher calorific value. The engine negation impact resulted in a minor reduction in BTE at full load.

3.1.2 Impact of injection time on HC and CO emission

Figures 8 and 9 shows the effect of IT on HC and CO emissions at 80 and 100% loads, respectively for a CRDI engine. Because the air-fuel mixture was of poor quality, the CGTSCPO20 fuel that was used to operate the CRDI engine produced more CO and HC emission than diesel. Since CGTSCPO20 has a heavier molecular structure, which leads to larger fuel particle sizes as a result, CGTSCPO20's poor combustion may be the cause of higher emissions at 600 bars. At 10° bTDC IT, the engine emission including CO and HC, were at their lowest level because of enhanced burning of fuel at a pressure of 600 bar.

On the other hand, incorrect combustion led to increased CO and HC emissions when using other types of fuel IT. Increased wall wetness in the combustion chamber is brought on by fuel injection timing that is advanced before 10° bTDC, while fuel injection timing that is retarded past 10° bTDC allows more fuel to be injected into the crevice, resulting in a loss of engine power. For CRDI operation at 10° bTDC, HC emissions for CGTSCPO20 and diesel fuels were 46 and 36 ppm, respectively, at 80% load. For CGTSCPO20 and diesel fuels, the corresponding values for CRDI mode at 10° bTDC are 60 and 50 ppm, respectively, at 100% load. At 80% load, CO emissions from CGTSCPO20 and diesel fuels in CRDI mode were 0.16 and 0.13%, respectively, at 10° bTDC. The percentages of CGTSCPO20 and diesel fuel consumption at full load are similarly low for a 10° bTDC system at 0.22 and 0.018 percent, respectively. However, CO and HC emission were enhanced at 10° bTDC IT using CGTSCPO20 and diesel at 600 bar with 7-hole CRDI injector and TRCC combustion chamber.

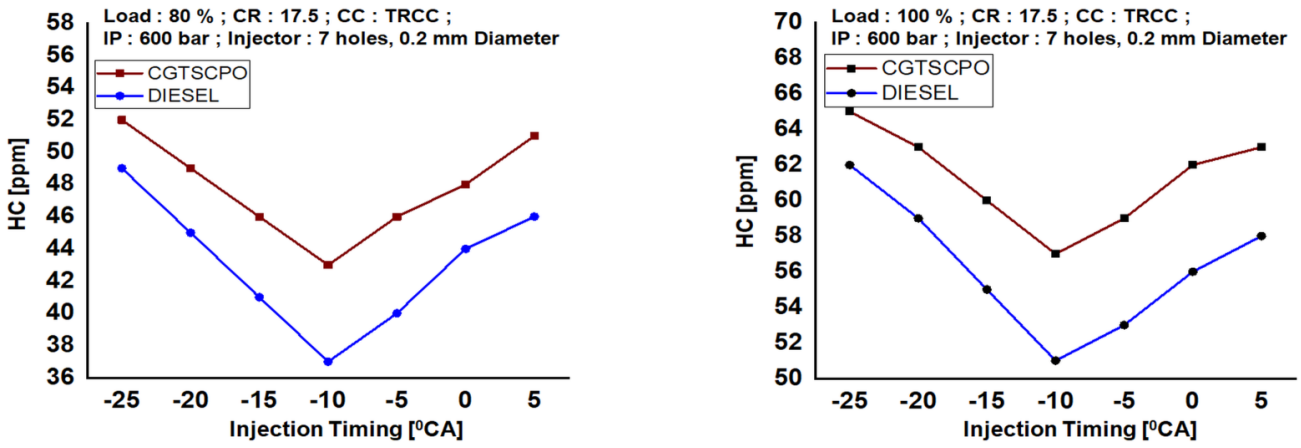

(a) (b)

Fig. 8. Variation in the HC for 80% and 100% load conditions at different ITs for diesel and CGTSCPO20.

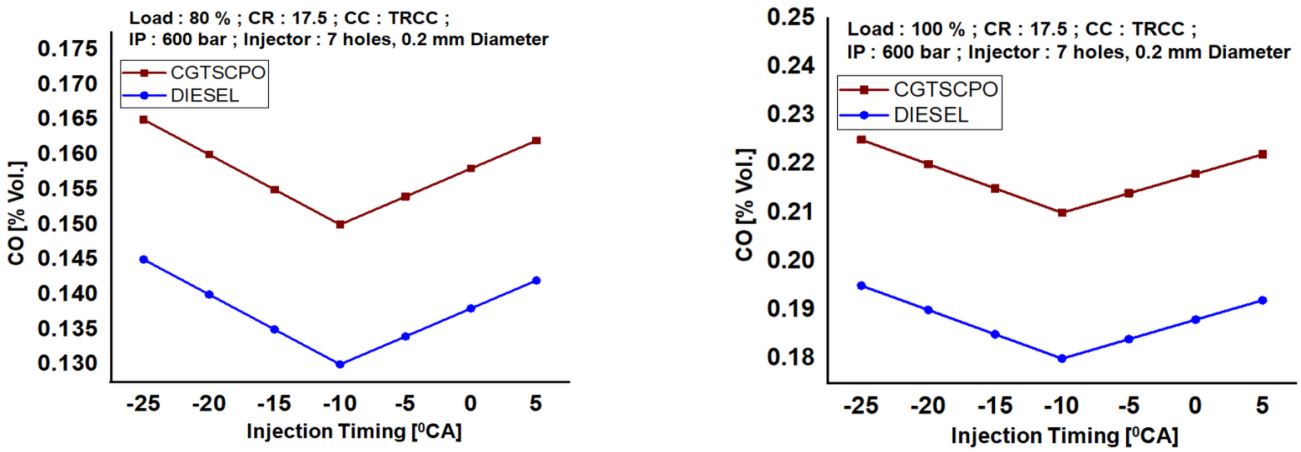

(a) (b)

Fig. 9. Variation in the CO for 80% and full load conditions at different ITs for diesel and CGTSCPO20.

3.1.3 Impact of injection time on NO_x

Figure 10 show the NO_x characteristics for CGTSCPO20 and diesel at 80% and full load, respectively. The flame temperature, the amount of time available for dwell, and the amount of oxygen present in the combustion chamber mixture were the primary factors influencing the formation of NO_x. When the engine is under load, the gas temperature inside the cylinder rises, causing the fuel injection rate to increase and, consequently, the amount of NO_x is created.

NO_x levels in CGTSCPO20 were lower than those of diesel. Some research suggests that its high latent heat of vaporisation is responsible for its low NO_x emissions. The CGTSCPO20's lower adiabatic temperature led to a cooler combustion temperature, which in turn reduced NO_x emissions. Less NO_x emissions are produced even though CGTSCPO20 has lower cetane number than diesel fuel due to lower exhaust gas temperature at 10° bTDC, 600 bar IOP, 7 hole CRDI injectors and TRCC combustion chamber shape.

3.1.4 Impact of injection time on smoke opacity

Figure 11 shows how injection timing affects the smoke opacity in CRDI engine running on diesel fuel and CGTSCPO20 at 80% and full load. There are a few reasons why the CRDI engine's diesel produces less smoke than a CGTSCPO20 engine, including the availability of oxygen, the availability of fuel-rich zones, and the involvement of incomplete combustion of hydrocarbons.

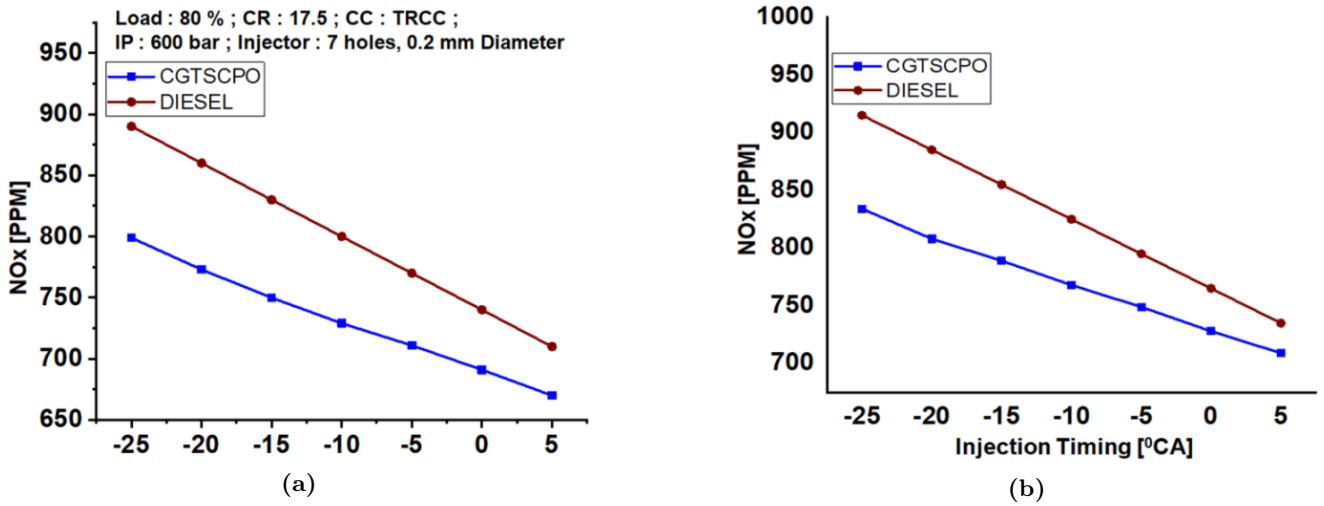

Fig. 10. Variation in the NO_x for 80% and full load conditions at different ITs for diesel and CGTSCPO20.

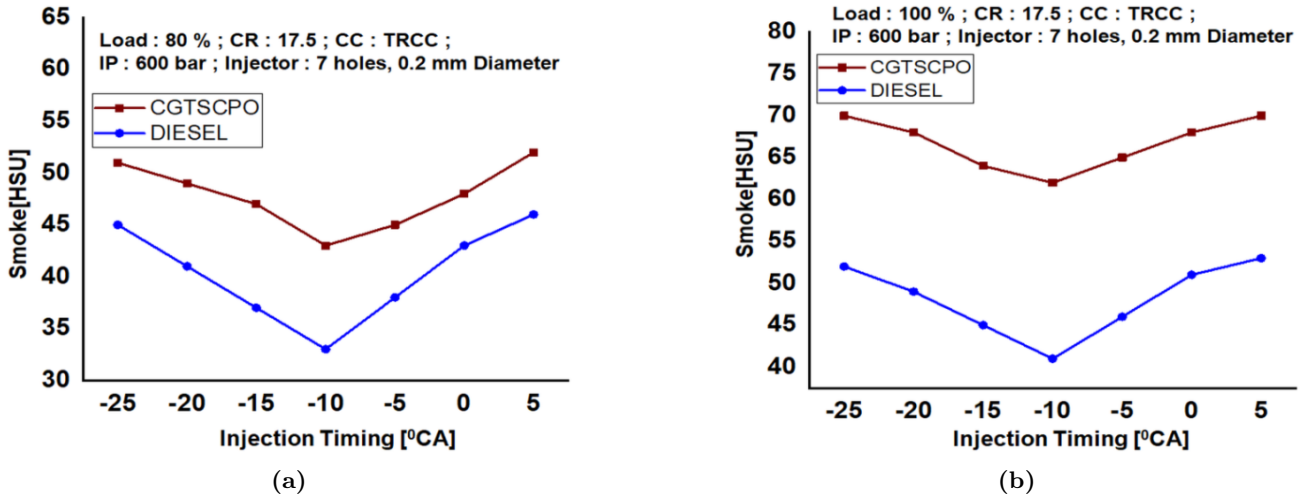

Fig. 11. Variation in the smoke for 80% and full load conditions at various ITs for diesel and CGTSCPO20.

CGTSCPO20's higher viscosity reduces the quality of mixing in the combustion chamber. The reduced wall wetness results in a declining trend in smoke levels for both fuels up to 10° bTDC at 600 bar. As a consequence of this, the process of combusting both fuels was enhanced, resulting in a higher BTE. However, a rise in smoke opacity was detected at 10° bTDC. This was due to a slower rate of air and fuel mixing, which in turn caused a slower rate of combustion. CGTSCPO20, on the other hand, generates a greater amount of smoke in a CRDI engine than diesel fuel due to higher viscous than diesel.

The smoke levels for CGTSCPO20 were on 80% load and at 10° bTDC, whereas the smoke levels for diesel were only 32 HSU. In a similar manner, the results that were obtained for CGTSCPO20 and diesel when operating at 100% load were 66 and 40 HSU, respectively. When using a CRDI engine with a 7-hole injector, a TRCC shaped combustion chamber, and 600 bar of in-cylinder pressure (IOP), the smoke intensity of CGTSCPO20 is 47 HSU, whereas the smoke levels for diesel were only 32 HSU.

In a similar manner, the results that were obtained for CGTSCPO20 and diesel when operating at 100% load were 66 and 40 HSU, respectively. When using a CRDI engine with a 7-hole injector, a TRCC-shaped combustion chamber, and 600 bar of in-cylinder pressure (IOP), the smoke intensity of CGTSCPO20 is higher than conventional diesel. This is because the diesel fuel burns quite totally than CGTSCPO20.

3.2 IOP optimization in CRDI engine for diesel and CGTSCPO20

With reference to results on previous section of the experiment, the CRDI engine running on CGTSCPO20 and diesel fuels was optimised for increased BTE and lower emissions at 80% load and 10° bTDC IT, under engine conditions that have a 7-hole CRDI injector, a constant IOP of 600 bar and a TRCC shape combustion chamber. However, CRDI engine performance when using alternate fuels was significantly affected by IOP variation. Hence, IOP ranged from 600 to 1100 bar for CGTSCPO20 and diesel fuels during the second part of the study was carried out at 10° CA bTDC while the optimal fuel IT remains constant.

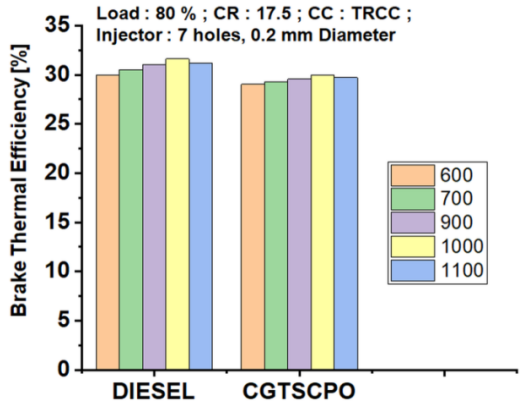

(a)

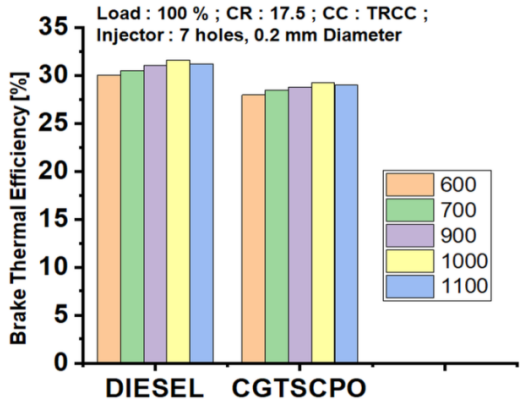

(b)

Fig. 12. Variation in the BTE for 80% and full load conditions at different IOPs for diesel and CGTSCPO20.

3.2.1 Effect of injector opening pressure on BTE

The effect of various IOP on the CRDI engine BTE at 80% and 100% load is depicted in Figure 12. Due to CGTSCPO20's higher viscosity, reduced volatility, lower cetane number, and negation effect resulting in poor atomization and thus poor combustion, CGTSCPO20 had a lower BTE than diesel for all IOPs selected for the study. The IOP has been increased from 600 to 1000 bar, rising the atomization of the spray characteristics. As a result, a homogeneous mixture is created in the combustion chamber, which can lead to shorter ignition delays and increased BTE at higher pressures. The viscosity of the fuel decreases as the injector pressure increases. Effective combustion takes place due to proper mixing of low viscous fuel with air. The BTE of the engine decreases at 1100 bar injector opening pressure for increased fuel leading to more wetting of wall. However, BTE reaches a maximum at IOP 1000 bar for increased fuel diffusion and fuel spreading in the cylinder.

3.2.2 Effect of injector opening pressure on HC and CO

Figures 13 and 14 illustrate the effect of IOP on HC and CO emissions from CGTSCPO20 and diesel fuel, respectively, when a CRDI engine was operating at 80% and 100% loads. High IOP was associated with lower HC and CO emissions among fuels and loads. This is because the fuel injected into the cylinder is more completely combusted and atomized. Lowered HC and CO emissions at 1000 bar IOP were associated with a higher oxygen concentration and an optimal burning rate during CGTSCPO20. However, CGTSCPO20 does have somewhat higher emissions than diesel in CRDI engines that could be due to the fuel's higher viscosity. Because of the increased wall wetting, the CO and HC emissions from the engine were greater at 1100 bar. The fuel spray that emerged from the combustion chamber across a greater pressure might be the cause of both the fuels and loads that were at higher pressure.

3.2.3 Effect of injector opening pressure on NO_x

Figure 15 illustrates the effect that varying levels of IOP have on the amount of NO_x emissions produced by CGTSCPO20 and diesel fuels while a CRDI engine is operating at 80% and 100% loads. Because of improvements made to the fuel's atomization and dispersion characteristics, the rate of combustion is accelerated. As a direct consequence of this, when the IOP of the fuel was raised, the temperature of the gases in the combustion chamber rises accordingly.

Due to its lower viscosity and density, diesel fuel produces a greater amount of nitrogen oxide emissions than CGTSCPO20 fuel does. According to the observed data, the engine's NO_x emission with

CGTSCPO20 fuel may be lower than with diesel fuel since the premixed combustion phase stage was shorter with CGTSCPO20 fuel than with diesel fuel. The CRDI engine's decreased NO_x emissions were a result of the combustion chamber's lower adiabatic flame temperature and the CGTSCPO20 oil's lower cetane number.

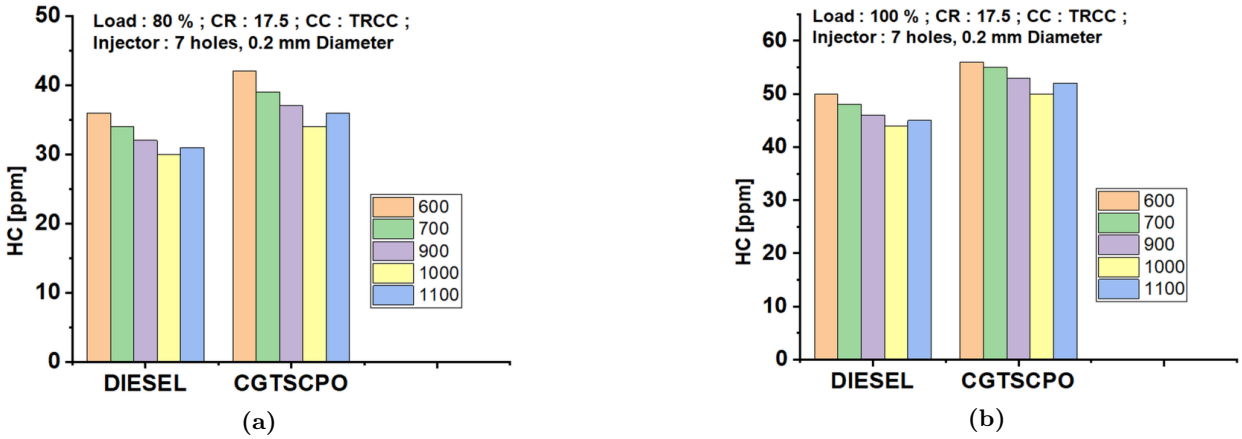

Fig. 13. Variation in the HC for 80% and full load conditions at various IOPs for diesel and CGTSCPO20.

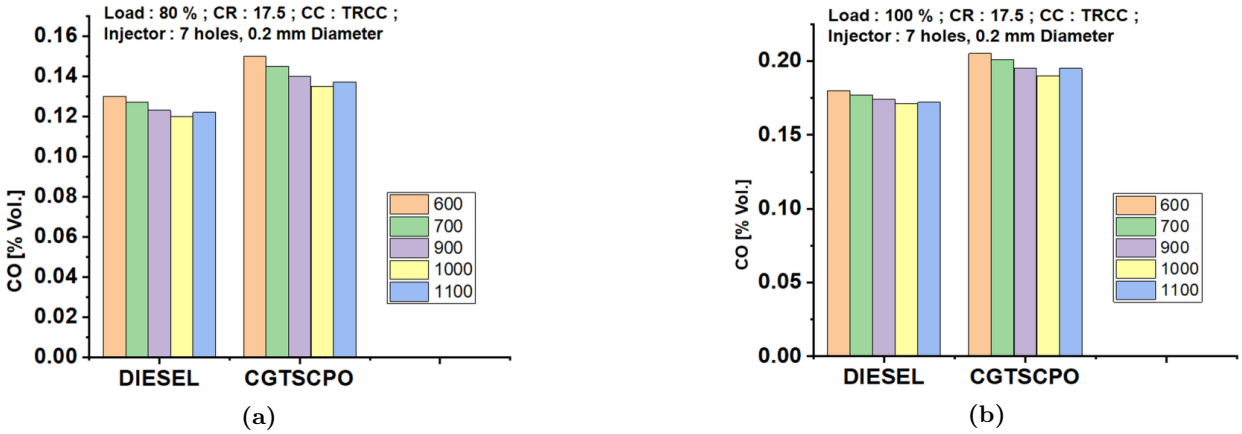

Fig. 14. Variation in CO for 80% and full load conditions at different IOPs for diesel and CGTSCPO20.

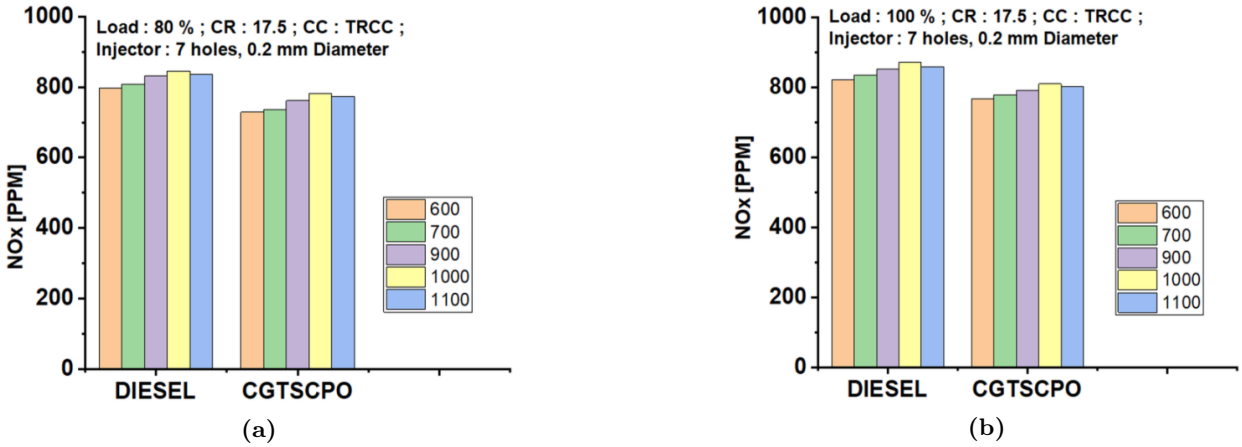

Fig. 15. Variation in the NO_x for 80% and full load conditions at different IOPs for diesel and CGTSCPO20.

3.2.4 Effect of injector opening pressure on smoke

Figure 16 depicts the smoke emission levels when the CRDI engine has been operated with CGTSCPO20 and diesel under the influence of IOP at 80% and full load, respectively. When the IOP was changed from 600 to 1000 bar, there was a reduction in smoke emission but when the IOP increased to 1100 bar, there was an increase in smoke effect for both CGTSCPO20 and diesel fuels. The minimum smoke level was measured at an IOP of 1000 bar. CGTSCPO20 produces more smoke than diesel for its high viscosity and molecular structure of more weight. The following are the optimal conditions that were determined after conducting tests on a CRDI engine operating at 80% and 100% of its rated capacity while subjected to the influence of an injection strategy. Maximum BTE was achieved at 80% load, 10° bTDC and 1000 bar. Furthermore, the lowest levels of nitrogen oxides, carbon monoxide, hydrocarbons, and smoke were recorded at 1000 bar when diesel and CGTSCPO20 fuels were used.

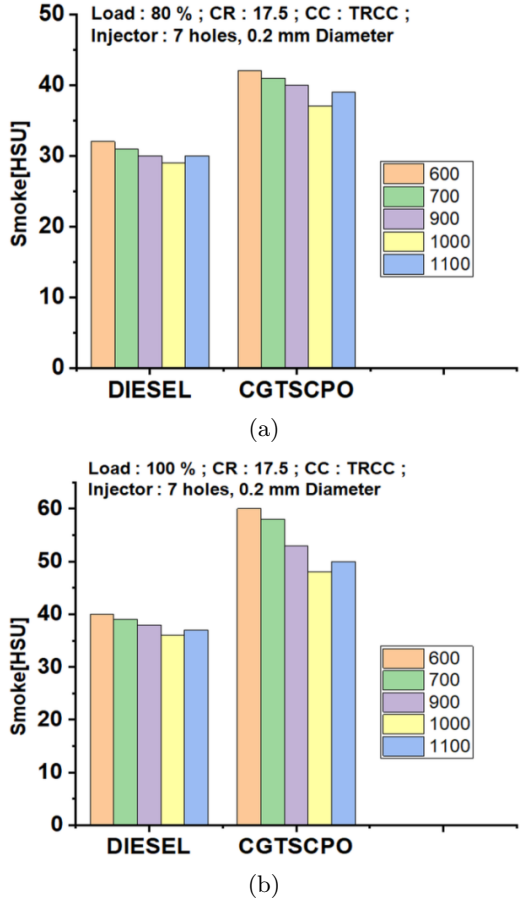

Fig. 16. Variation in the smoke for 80% and full load conditions at different IOPs for diesel and CGTSCPO20.

3.3 Thermodynamic analysis

3.3.1 The 1st law thermodynamic analysis (energy analysis)

Figures 17 and 18 show the energy flow diagrams (Sankey diagrams) for diesel and CGTSCPO20 fuelled engine, respectively, under optimal MIS conditions. Under optimal conditions, 30.55% of the energy in diesel fuel is converted to output power, 19.76% is lost as heat to cooling water, 22% is lost as heat to exhaust gases, and the remaining 27.77% is lost in other ways (friction losses, heat transfer loss, etc.) from diesel. In CGTSCPO20, a similar energy distribution pattern is seen at optimal levels by converting a substantial proportion of the inlet energy (fuel energy) into output power, which is little lower compared to diesel at about 29.73%. Since biodiesel fuel has a lower calorific value than conventional diesel fuel, CGTSCPO20 has a lower power output than diesel fuel under optimal conditions. Several variables, including fuel molar fraction, combustion products, and enthalpy change, affect the energy fraction of a percent of heat transfer.

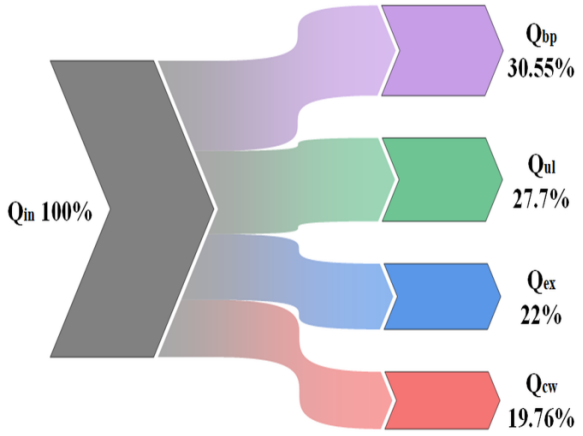

Fig. 17. Sankey diagram for diesel.

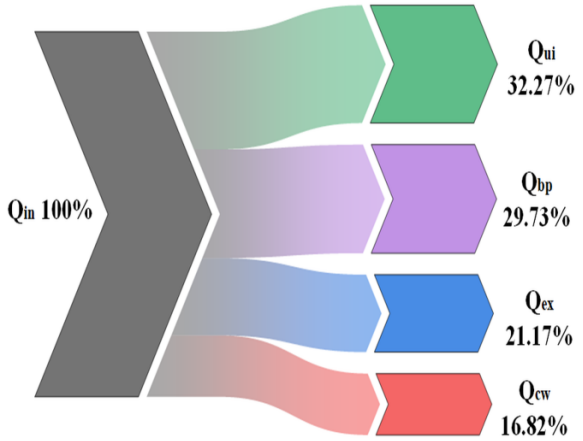

Fig. 18. Sankey diagram for CGTSCPO20.

CGTSCPO20 had a 32.27% heat rejection in other ways. Several variables, including fuel molar fraction, combustion products, and enthalpy change, affect the energy fraction of the heat transfer percentage. CGTSCPO20 has a heat rejection of 32.27% as the other ways. At this rate of heat loss, about one-third of the total fuel energy is lost. Heat rejection to the environment is the major contributor to energy intake for all fuels. About 48% of the energy from fuel is lost as waste heat. Exhaust energy and cooling water rates for CGTSCPO20 have remained at 16.82% and 21.17%, respectively, under optimal MIS conditions. The rate at which the heat energy of the exhaust gases is dissipated is referred to as the exhaust energy rate. When compared across fuel types, the exhaust energy rate showed very little to almost no noticeable change. Figure 19 depicts a comparison between the energy distribution of diesel and CGTSCPO20.

3.3.2 The 2nd law thermodynamic analysis

Exergy analysis was conducted in relation to system irreversibility or destruction, input air and fuel, exhaust gas losses, output power, and heat loss. Exergy flow (Grassmann) diagrams for the diesel-fuelled engine and the CGTSCPO20 engine, respectively, are shown in Figures 19 and 20. While the net exergy work of 29.57% and 28.46% is produced for diesel and CGTSCPO20 fuels, respectively, both 4.27% and 2.7% were lost through cooling water. Both fuels' exergy work rates at optimum conditions were at least greater than their input energy.

An important part of the exergy from the test fuels that was transferred to the engine was destroyed as a result of system Irreversibility. Experimental results showed that CGTSCPO20 had greater exergy destruction than diesel fuel. When the conditions for comparing the two fuels are at optimal MIS, the diesel fuel has higher exhaust exergy than the CGTSCPO20 fuel in terms of the exergy percentage of the exhaust gas. The exhaust exergy rate of the diesel engine is 15.99%, while that of the CGTSCPO20 is 9.6%. This may be due to the high viscosity and low calorific value of CGTSCPO20.

It may be found that the exergy for heat transfer is only the same for the two fuels and that the average exergy for heat transfer is about 5% of the exergy that was input to the engine. High oxygen content increases combustion, which raises cylinder temperature and increases cooling water loss. The increased oxygen concentration in CGTSCPO20 accounts for its higher heat transfer exergy than diesel fuel. The fuel exergy, also known as the input exergy, is affected by factors such as flow rate of mass, the lower calorific value and the chemical exergy factor along with other factors. A similar type of behaviour is observed between exergy and fuel energy. Rate of exergy was found to be more than rate of energy of fuel because the chemical exergy factor is more than one. The exergy destruction percentage accounts for the vast majority of the total input exergy in an exergy study. Diesel and CGTSCPO20 fuels have exergy destruction rates of 50.17% and 59.24%, respectively. Fuel type had no impact on the irreversibility or energy destruction fraction. Figure 20 illustrates the comparison of exergy distributions for diesel and CGTSCPO20.

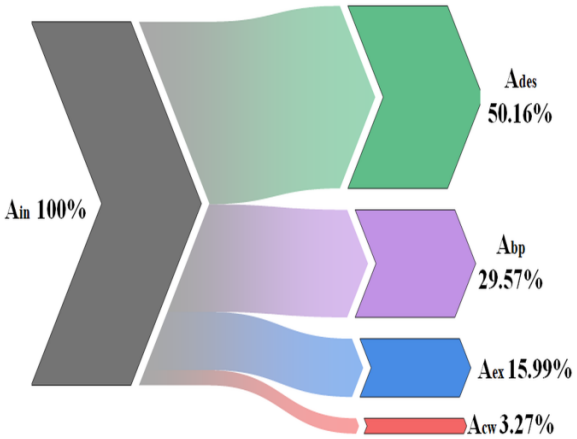

Fig. 19. Grassmann diagram (diesel).

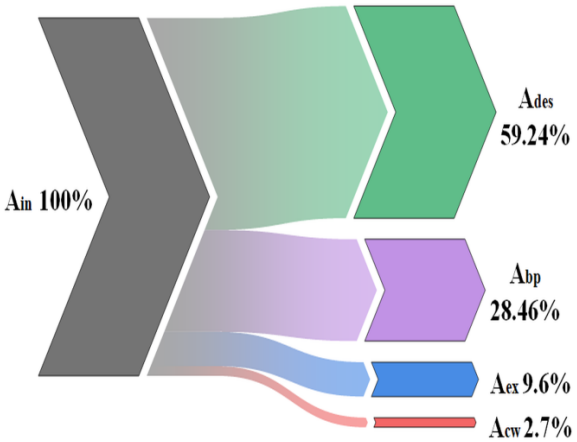

Fig. 20. Grassmann diagram (CGTSCPO20).

4 Conclusions

In order to enable various IT and IOP, the single-cylinder CI engine employed in this study was appropriately adapted to run in CRDI mode. The impact of IT and IOP on the performance of a CRDI engine running on diesel and CGTSCPO20 was investigated experimentally at a range of fuel injector pressures (600,

700, 800, 1000, and 1100 bar), timings (−25° bTDC to +5° aTDC with a 5° step), and loads (80% and 100%), while all keeping the engine running at a constant 1500 RPM. Fuel energy rate, net-work rate, heat loss rate through exhaust gas, cooling water as well as fuel and exhaust exergy rates, heat transfer exergy rates, and exergy destruction of CRDI engines operated with diesel and CGTSCPO20 were compared with each other under ideal fuel injection timing, fuel injector pressure, and constant speed conditions. According to the study's findings, the following conclusions can be drawn:

- The measured fuel properties of CGTSCPO20 comply with the standards of ASTM D6751 and EN 14214.
- According to the research findings, the results obtained on energy efficiencies is not sufficient to determine which engines have the best performance. In addition to the energy analysis, an exergy analysis can also be carried out for the control volume, which can lead to more accurate and realistic findings than the energy analysis alone.
- For greater engine brake thermal efficiency, the 80% engine load was optimised.
- The BTE showed a rising trend with retarded IT up to 10° bTDC for a CGTSCPO20 fuelled CRDI engine; however, after reaching this point, the BTE began to decrease. When compared to diesel, CGTSCPO20 demonstrated poor performance in terms of lower BTE levels.
- In contrast to CO and smoke emissions, which significantly decreased up to 10° bTDC and increased after the indicated IT, HC emissions decreased with IT was retarded. But as usual, NO_x emissions increase with advanced IT.
- When the IP was increased, the BTE increased as well, but once it reached 1000 bar, the BTE began to decrease.
- For both loads of 80 and full load, HC and CO emissions exhibited comparable patterns, with minimal values at 1000 bar. When the pressure reached 1000 bar, these emissions increased.
- An increase in IOP was accompanied by a corresponding increase in NO_x emissions.
- The CRDI diesel engine's optimized parameters led to increased BTE and reduced emissions when operating with the following engine settings: 1000 bar IOP, 10° bTDC fuel IT, and a TRCC shaped combustion chamber with a CR constant of 17.5 and the engine was run on CGTSCPO20 as an alternate fuel at 80% load.
- At optimal settings, it observed the exergy destructions of 6.82 kW for a diesel-fuelled engine and 8.43 kW for a CGTSCPO20 fuelled one.
- The primary factor contributing to system inefficiency is the destruction of energy resulting from irreversible processes like combustion. Other variables that lower exergy efficiency include exergy lost through heat transfer, cooling water, and exhaust system.

As a whole, it can be concluded that modified CRDI single-cylinder CI engines performed well with CGTSCPO20, similar to operations with pure diesel. This experimental study shows that CGTSCPO20 can be used as an alternative fuel for diesel.

4.1 Future research scope

It is suggested that further research can be carried out on the topic of investigating the impacts of CGTSCPO20 and diesel blends, as well as the various operating circumstances of the engine, such as engine speed, CR, EGR, and other factors on the energy and exergy studies.

Declarations

Availability of data and material Due to experimental nature of research, authors confirm that the data supporting the findings of this study are available within the article.

Conflict of interest No potential conflict of interest was reported by the authors.

Funding Authors declare that no funding has been received from any organization/ funding source as research assistance for current research.

Authors' contributions Each author has equal contributions in analyzing, writing, editing, formatting, experimenting and finalizing this research and contributed equal effort to bring success in preparation of this manuscript. All authors have read and approved the manuscript.

Acknowledgements The authors are highly thankful to Jawaharlal Nehru Technological university, Anantapur, Andhra Pradesh, India, for providing all kinds of research support in data analysis, experimental findings and development of this new research.

Nomenclature

aTDC	After top dead center
BSFC	Brake specific fuel consumption
bTDC	Before top dead center

BTE	Brake thermal efficiency
CGTSCPO	Congress grass tamarind shell co-pyrolysis oil
CO	Carbon monoxide
CRDI	Common rail direct injection
CV	Calorific value
C_w	Specific heat of cooling water in kJ/kgK
ECU	Electronic control unit
HC	Hydro carbon
IOP	Injector Opening Pressure
IT	Injection Timing
LCV	Lower Calorific value of fuel in kJ/kg
m_f	mass of fuel in kg
MIS	Multiple injection strategies
m_w	mass of water (kg)
N	Speed in RPM
NO_x	Nitrogen oxides
PM	Particulate matter
Q_{bp}	Heat equivalent to Brake power in kJ
Q_i	Input Heat Energy in kJ
Q_w	Heat carried away by Cooling Water (kJ)
SOI	Start of injection
T	Torque in $\mathrm{N \cdot m}$
TRCC	Toroidal re-entrant combustion chamber
T_{wi}	Temperature of cooling water at inlet in K

References

[1] Senthil Kumar M. Experimental investigations on the efficient use of vegetable oils in diesel engines; 2003.

[2] Laksmono N, Paraschiv M, Loubar K, Tazerout M. Biodiesel production from biomass gasification tar via thermal/catalytic cracking. Fuel processing technology. 2013;106:776–783.

[3] Appels L, Lauwers J, Degrève J, Helsen L, Lievens B, Willems K, et al. Anaerobic digestion in global bio-energy production: potential and research challenges. Renewable and Sustainable Energy Reviews. 2011;15(9):4295–4301.

[4] Toor SS, Rosendahl L, Rudolf A. Hydrothermal liquefaction of biomass: A review of subcritical water technologies. Energy. 2011;36(5):2328–2342.

[5] Demirbas A, Arin G. An overview of biomass pyrolysis. Energy sources. 2002;24(5):471–482.

[6] Mohan D, Pittman Jr CU, Steele PH. Pyrolysis of wood/biomass for bio-oil: a critical review. Energy & fuels. 2006;20(3):848–889.

[7] Chen W, Shi S, Zhang J, Chen M, Zhou X. Co-pyrolysis of waste newspaper with high-density polyethylene: Synergistic effect and oil characterization. Energy Conversion and Management. 2016;112:41–48.

[8] Ferrara F, Orsini A, Plaisant A, Pettinau A. Pyrolysis of coal, biomass and their blends: Performance assessment by thermogravimetric analysis. Bioresource technology. 2014;171:433–441.

[9] Guan Y, Ma Y, Zhang K, Chen H, Xu G, Liu W, et al. Co-pyrolysis behaviors of energy grass and lignite. Energy conversion and management. 2015;93:132–140.

[10] Ben H, Ragauskas AJ. Comparison for the compositions of fast and slow pyrolysis oils by NMR characterization. Bioresource technology. 2013;147:577–584.

[11] Dong Cq, Zhang Zf, Lu Q, Yang Yp. Characteristics and mechanism study of analytical fast pyrolysis of poplar wood. Energy conversion and Management. 2012;57:49–59.

[12] Capunitan JA, Capareda SC. Assessing the potential for biofuel production of corn stover pyrolysis using a pressurized batch reactor. Fuel. 2012;95:563–572.

[13] Park YK, Yoo ML, Lee HW, Park SH, Jung SC, Park SS, et al. Effects of operation conditions on pyrolysis characteristics of agricultural residues. Renewable Energy. 2012;42:125–130.

[14] Pattiya A, Sukkasi S, Goodwin V. Fast pyrolysis of sugarcane and cassava residues in a free-fall reactor. Energy. 2012;44(1):1067–1077.

[15] Pattiya A, Suttibak S. Production of bio-oil via fast pyrolysis of agricultural residues from cassava plantations in a fluidised-bed reactor with a hot vapour filtration unit. Journal of Analytical and Applied Pyrolysis. 2012;95:227–235.

[16] Bhaskar T, Bhavya B, Singh R, Naik DV, Kumar A, Goyal HB. Thermochemical conversion of biomass to biofuels. In: Biofuels. Elsevier; 2011. p. 51–77.

[17] Rakopoulos C, Giakoumis E. Comparative first- and second-law parametric study of transient diesel engine operation. Energy. 2006;31(12):1927–1942.

[18] Rakopoulos CD, Kyritsis DC. Comparative second-law analysis of internal combustion engine operation for methane, methanol, and dodecane fuels. Energy. 2001;26(7):705–722.

[19] Rosen MA, Dincer I. Exergy as the confluence of energy, environment and sustainable development. Exergy, an International journal. 2001;1(1):3–13.

[20] Van Gerpen JH, Shapiro HN. Second-Law Analysis of Diesel Engine Combustion. Journal of Engineering for Gas Turbines and Power. 1990 01;112(1):129–137. Available from: https://doi.org/10.1115/1.2906467.

[21] Zheng J, Caton JA. Second law analysis of a low temperature combustion diesel engine: effect of injection timing and exhaust gas recirculation. Energy. 2012;38(1):78–84.

[22] Caliskan H, Tat ME, Hepbasli A, Van Gerpen JH. Exergy analysis of engines fuelled with biodiesel from high oleic soybeans based on experimental values. International Journal of Exergy. 2010;7(1):20–36.

[23] Canakci M, Hosoz M. Energy and exergy analyses of a diesel engine fuelled with various biodiesels. Energy Sources, Part B. 2006;1(4):379–394.

[24] da Costa YJR, de Lima AGB, Bezerra Filho CR, de Araujo Lima L. Energetic and exergetic analyses of a dual-fuel diesel engine. Renewable and Sustainable Energy Reviews. 2012;16(7):4651–4660.

[25] López I, Quintana C, Ruiz J, Cruz-Peragón F, Dorado M. Effect of the use of olive–pomace oil biodiesel/diesel fuel blends in a compression ignition engine: Preliminary exergy analysis. Energy conversion and Management. 2014;85:227–233.

[26] Sekmen P, Yılbaşı Z. Application of energy and exergy analyses to a CI engine using biodiesel fuel. Mathematical and Computational Applications. 2011;16(4):797–808.

[27] Debnath BK, Sahoo N, Saha UK. Thermodynamic analysis of a variable compression ratio diesel engine running with palm oil methyl ester. Energy Conversion and Management. 2013;65:147–154.

[28] Panigrahi N, Mohanty M, Acharya S, Mishra S, Mohanty R. Experimental investigation of karanja oil as a fuel for diesel engine-using shell and tube heat exchanger. World Academy of Science, Engineering and Technology, International Journal of Chemical, Materials Science and Engineering. 2014;8(1):91–98.

[29] Panigrahi N, Mohanty MK, Mohanty RC, Mishra SR. Performance of a CI engine with energy and exergy analysis fuelled with neem oil methyl ester. International Journal of Renewable Energy Technology. 2016;7(3):264–287.

[30] Karagoz M, Uysal C, Agbulut U, Saridemir S. Exergetic and exergoeconomic analyses of a CI engine fueled with diesel-biodiesel blends containing various metal-oxide nanoparticles. Energy. 2021;214:118830.

[31] Karami S, Gharehghani A. Effect of nano-particles concentrations on the energy and exergy efficiency improvement of indirect-injection diesel engine. Energy Reports. 2021;7:3273–3285.

[32] Nabi MN, Rasul M. Influence of second generation biodiesel on engine performance, emissions, energy and exergy parameters. Energy conversion and management. 2018;169:326–333.

[33] Nemati P, Jafarmadar S, Taghavifar H. Exergy analysis of biodiesel combustion in a direct injection compression ignition (CI) engine using quasi-dimensional multi-zone model. Energy. 2016;115:528–538.

[34] Sarıkoç S, Örs İ, Ünalan S. An experimental study on energy-exergy analysis and sustainability index in a diesel engine with direct injection diesel-biodiesel-butanol fuel blends. fuel. 2020;268:117321.

[35] Şanli BG, Uludamar E. Energy and exergy analysis of a diesel engine fuelled with diesel and biodiesel fuels at various engine speeds. Energy Sources, Part A: Recovery, Utilization, and Environmental Effects. 2020;42(11):1299–1313.

[36] Yesilyurt MK, Arslan M. Analysis of the fuel injection pressure effects on energy and exergy efficiencies of a diesel engine operating with biodiesel. Biofuels. 2018;.

[37] Agarwal AK, Dhar A, Gupta JG, Kim WI, Choi K, Lee CS, et al. Effect of fuel injection pressure and injection timing of Karanja biodiesel blends on fuel spray, engine performance, emissions and combustion characteristics. Energy Conversion and Management. 2015;91:302–314.

[38] Jiaqiang E, Pham M, Deng Y, Nguyen T, Duy V, Le D, et al. Effects of injection timing and injection pressure on performance and exhaust emissions of a common rail diesel engine fueled by various concentrations of fish-oil biodiesel blends. Energy. 2018;149:979–989.

[39] Kanth S, Ananad T, Debbarma S, Das B. Effect of fuel opening injection pressure and injection timing of hydrogen enriched rice bran biodiesel fuelled in CI engine. International Journal of Hydrogen Energy. 2021;46(56):28789–28800.

[40] Khandal S, Banapurmath N, Gaitonde V. Effect of hydrogen fuel flow rate, fuel injection timing and exhaust gas recirculation on the performance of dual fuel engine powered with renewable fuels. Renewable energy. 2018;126:79–94.

[41] Jayaraman J, Reddy S, et al. Effects of injection pressure on performance & emission characteristics of CI engine using graphene oxide additive in bio-diesel blend. Materials Today: Proceedings. 2021;44:3716–3722.

[42] Stone R. Introduction to internal combustion engines. vol. 3. Springer; 1999.

[43] Shinde AB, Umadi OA, Gawali SV, Kamble A. Common Rail Direct Injection. International Research Journal of Engineering and Technology. 2020;7(4):3095–3102.

[44] Indrareddy N, Venkateswarlu K, Konijeti R. Experimental investigation of algae biofuel–diesel blends on performance of a CRDI diesel engine. International Journal of Ambient Energy. 2022;43(1):2218–2225.

[45] Aalam CS, Saravanan C, Kannan M. Experimental investigations on a CRDI system assisted diesel engine fuelled with aluminium oxide nanoparticles blended biodiesel. Alexandria engineering journal. 2015;54(3):351–358.

[46] Khandal S, Banapurmath N, Gaitonde V. Effect of exhaust gas recirculation, fuel injection pressure and injection timing on the performance of common rail direct injection engine powered with honge biodiesel (BHO). Energy. 2017;139:828–841.

[47] Ashok B, Nanthagopal K, Saravanan B, Somasundaram P, Jegadheesan C, Chaturvedi B, et al. A novel study on the effect lemon peel oil as a fuel in CRDI engine at various injection strategies. Energy conversion and management. 2018;172:517–528.

[48] Duda K, Wierzbicki S, Śmieja M, Mikulski M. Comparison of performance and emissions of a CRDI diesel engine fuelled with biodiesel of different origin. Fuel. 2018;212:202–222.

[49] Roy S, Ghosh A, Das AK, Banerjee R. A comparative study of GEP and an ANN strategy to model engine performance and emission characteristics of a CRDI assisted single cylinder diesel engine under CNG dual-fuel operation. Journal of natural gas science and engineering. 2014;21:814–828.

[50] Rath M, Acharya S. Exergy and energy analysis of diesel engine using karanja methyl ester under varying compression ratio. International Journal of Engineering. 2014;27(8):1259–1268.

[51] Rath MK, Mohanta DK. Exergy and energy analysis of compression ignition engine using diesel and karanja oil blends under varying compression ratio and engine load. Biofuels. 2023;14(2):173–182.